

Supporting Information

Regulating Molecular Packing and Crystallization Kinetics via Trifluoromethyl-Functionalized Solid Additives for Efficient Organic Solar Cells

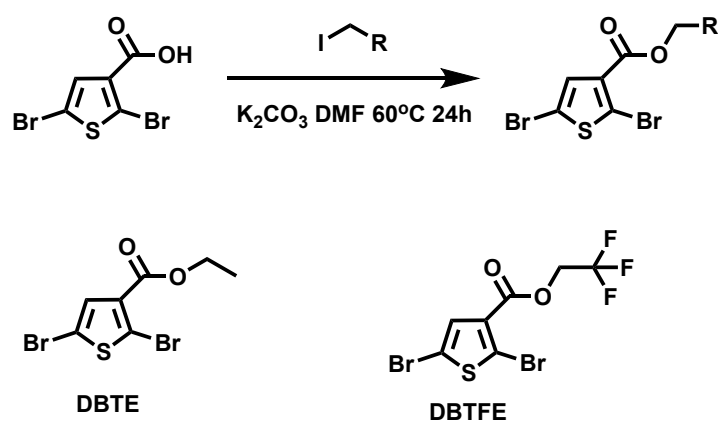
Jiang Zhou,^a Wenzhao Xiong,^a Zhaohan Chai,^b Duozi Gu,^a Yunxi Xu,^a Zhibo Wang,^a Shenbo Zhu,^a Yongjie Cui,^{*b} Huawei Hu^{*a}

^aState Key Laboratory of Advanced Fiber Materials, College of Materials Science and Engineering, Donghua University, Shanghai 201620, China, E-mail: huawei.hu@dhu.edu.cn

^bSchool of Energy and Materials, Shanghai Polytechnic University, Shanghai 201209, China, E-mail: yjcui@sspu.edu.cn

1. Materials. The polymer donor PM6 was purchased from Volt-Amp Optoelectronics Tech. Co., Ltd. The acceptor Y6, L8-BO and BET-eC9 were purchased from eFlexPV Limited. PEDOT:PSS (Clevios PVP A14083) was purchased from Heraeus Inc.

2. Synthesis of Additives



Scheme S1. The synthetic route of DBTE and DBTFE.

Synthesis of compound DBTE: The iodoethane (653.5 mg, 4.19 mmol) was added to a solution of 2, 5-dibromothiophene-3-carboxylic acid (300 g, 1.05 mmol) and potassium carbonate (578.2 mg, 4.19 mmol) in DMF (10 mL). The reaction was stirred at 60 °C for ten hours. After cooling to room temperature, the mixture was extracted by dichloromethane/water. The solvent was removed under reduced pressure, and the crude produced was purified by silica gel column chromatography. The product was obtained as white solid (286mg, 87%). ¹H NMR (600 MHz, CDCl₃) δ 7.35 (s, 1H), 4.33 (q, 2H), 1.37 (d, 3H).

Synthesis of compound DBTFE: 3-Fluoroethyl iodide (880.3 mg, 4.19 mmol) was added to a solution of 2, 5-dibromothiophene-3-carboxylic acid (300 g, 1.05 mmol) and potassium carbonate (578.2 mg, 4.19 mmol) in DMF (10 mL). The reaction was stirred at 60 °C for ten hours. After cooling to room temperature, the mixture was extracted by dichloromethane/water. The solvent was removed under reduced pressure, and the crude produced was purified by silica gel column chromatography. The product was

obtained as white solid (262mg, 68%). $^1\text{H NMR}$ (600 MHz, CDCl_3) δ 7.39 (s, 1H), 4.64 (q, 2H).

3. Experimental Section

Device fabrication. OSCs were made with a device structure of ITO/PEDOT:PSS /polymer:acceptor /PDINN/Ag. The patterned ITO-coated glass was wiped with a lint-free cloth soaked in a cleaning agent, then subjected to ultrasonic cleaning using deionized water, acetone, and isopropanol solvents. The substrate should undergo ultraviolet-ozone treatment before use. Place the cleaned substrate in a UVO zone Cleaner for 20 minutes. A thin PEDOT:PSS layer with a thickness of about 40 nm was spin-coat onto the ITO substrates at 4000 rpm for 40 s, and then dried at 150 °C for 15 min in air. The various blend systems including PM6:Y6 (15.4 mg ml⁻¹, 1:1.2 wt/wt), and PM6:Y6:additive (15.4 mg ml⁻¹, 1:1.2:0.1wt/wt) were dissolved in chloroform. Then, all solutions were stirred for 2 h. Next, the active layer was spin-coated on the PEDOT:PSS layer. The active layer was further annealed under 100 °C for 10 min. Subsequently, the PDINN cathode interface layer was spin-coated onto the active layer at 3000 rpm for 30 s. The 100 nm Ag was thermally deposited in a vacuum chamber at a pressure of 5×10^{-5} Pa through a shadow mask.

4. Instruments and Measurement

Optical characterization. The J - V characteristics were measured by Keithley 2400 Source Meter under 1 simulator solar light (100 mW/cm², AM 1.5 G). The EQE spectra were recorded on a commercial EQE measurement system (Enlitech, QE-S EQE). UV-vis absorption spectra were measured by Perkin Elmer Lambda 20 UV/VIS spectrophotometer.

Film-depth-dependent absorption spectroscopy. Film-depth-dependent light absorption spectra were acquired by a spectrometer (PU100, Shaanxi Puguang Weishi Co. Ltd.) (Shaanxi, China) equipped with a soft plasma-ion source. The power-supply for generating the soft ionic source was 100 W with an input oxygen pressure ~ 10 Pa.

The film surface was incrementally etched by the soft ion source, without damage to the materials underneath the surface, which was in situ monitored by a spectrometer. From the evolution of the spectra and the Beer–Lambert’s Law, film-depth-dependent absorption spectra were extracted. The composition distribution along the film-depth direction was obtained from the film-depth-dependent spectra by fitting the sub-layer absorption using the absorption of the pure components. The exciton generation contour is numerically simulated upon inputting sub-layer absorption spectra into a modified optical transfer-matrix approach.

AFM characterization. AFM measurements were performed by using a Scanning Probe Microscope Dimension 3100 in tapping mode. All film samples were spin-cast on ITO substrates.

Intermolecular interactions measurement. Contact angle measurements were carried out by an Attension Theta Flex meter, using water and ethylene glycol by sessile drop analysis. The surface tension values of films are calculated according to the previous report, in which:

$$\begin{aligned} \gamma_{\text{water}}(\text{COS}\theta_{\text{water}}+1) &= \frac{4\gamma_{\text{water}}^p \times \gamma^p}{\gamma_{\text{water}}^p + \gamma^p} + \frac{4\gamma_{\text{water}}^d \times \gamma^d}{\gamma_{\text{water}}^p + \gamma^d} \\ \gamma_{\text{EG}}(\text{COS}\theta_{\text{EG}} + 1) &= \frac{4\gamma_{\text{EG}}^p \times \gamma^p}{\gamma_{\text{EG}}^p + \gamma^p} + \frac{4\gamma_{\text{EG}}^d \times \gamma^d}{\gamma_{\text{EG}}^p + \gamma^d} \end{aligned}$$

$$\gamma = \gamma^d + \gamma^p$$

where θ is the contact angle of each thin film, and γ is the surface tension of samples, which is equal to the sum of the dispersion (γ^d) and polarity (γ^p) components; γ_{water} and γ_{EG} are the surface tensions of the water and ethylene glycol; and γ_{water}^d , γ_{water}^p , γ_{EG}^d and γ_{EG}^p are the dispersion and polarity components of γ_{water} and γ_{EG} . The Flory-Huggins interaction parameters are deduced from:

$$\chi^{D-A} = K(\sqrt{\gamma^D} - \sqrt{\gamma^A})^2, \text{ where } K \text{ is a positive constant at a specific temperature.}$$

GIWAXS characterization: Samples were prepared on Si substrates using identical

blend solutions like those used in devices. The 10 keV X-ray beam was incident at a grazing angle of 0.11°-0.15°, which maximized the scattering intensity from the samples. In-plane and out-of-plane sector averages were calculated using the Nika software package. The uncertainty for the peak fitting of the GIWAXS data is 0.3 Å. The coherence length was calculated using the Scherrer equation: $CCL = 2\pi K/\Delta q$, where Δq is the full-width at half-maximum of the peak and K is a shape factor (0.9 was used here).

Transient photovoltage (TPV) and transient photocurrent (TPC) measurements.

In TPV measurements, the devices were placed under background light bias enabled by a focused Quartz Tungsten-Halogen Lamp with an intensity of similar to working devices, i.e., the device voltage matches the open-circuit voltage under solar illumination conditions. Photo-excitations were generated with an 8 ns pulses from a laser system (Oriental Spectra, NLD520). The wavelength for the excitation was tuned to 518 nm with a spectral width of 3 nm. A digital oscilloscope was used to acquire the TPV signal at the open-circuit condition. TPC signals were measured under short-circuit conditions under the same excitation wavelength without background light bias. The TPV and TPC decay curves were fitted with a single exponential function, and the decay constants were obtained from the fitting.

DFT Calculation. Geometry optimizations were carried out by the density functional theory (DFT) method at the B3LYP-D3BJ/6-31G(d,p) level. All the calculations were performed using Gaussian 16 program.

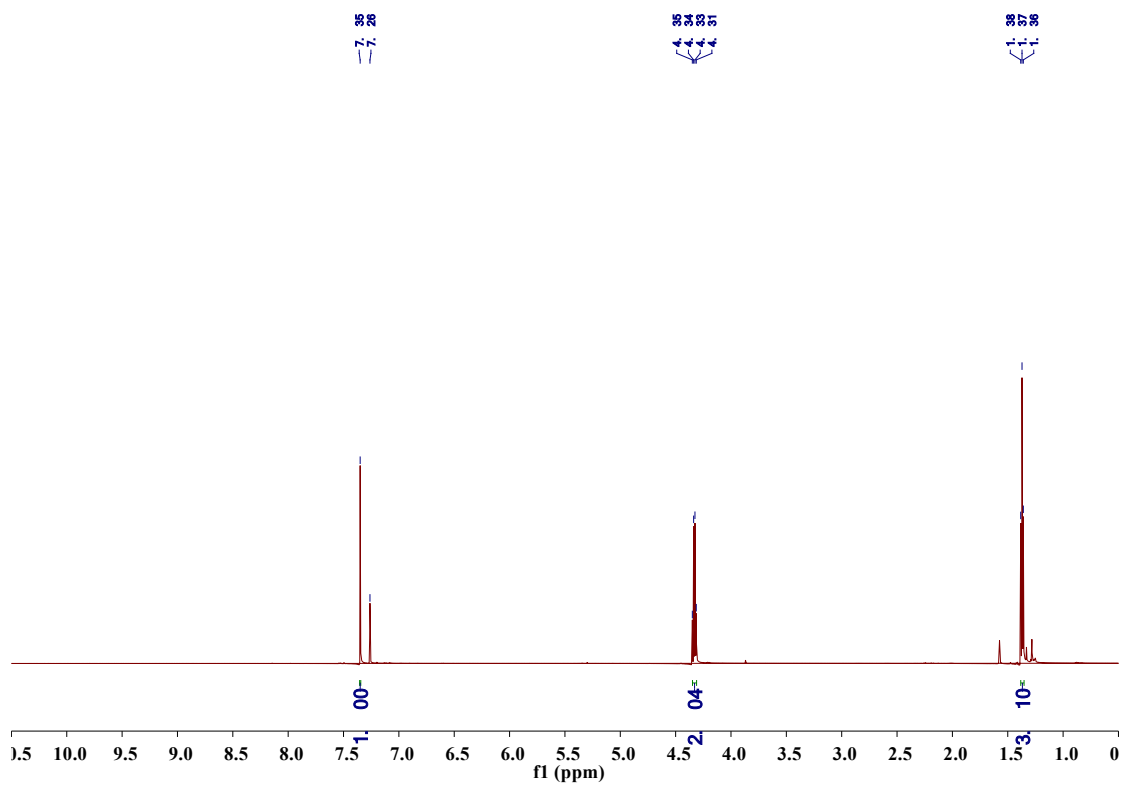


Figure S1. ¹H NMR spectrum of DBTFE.

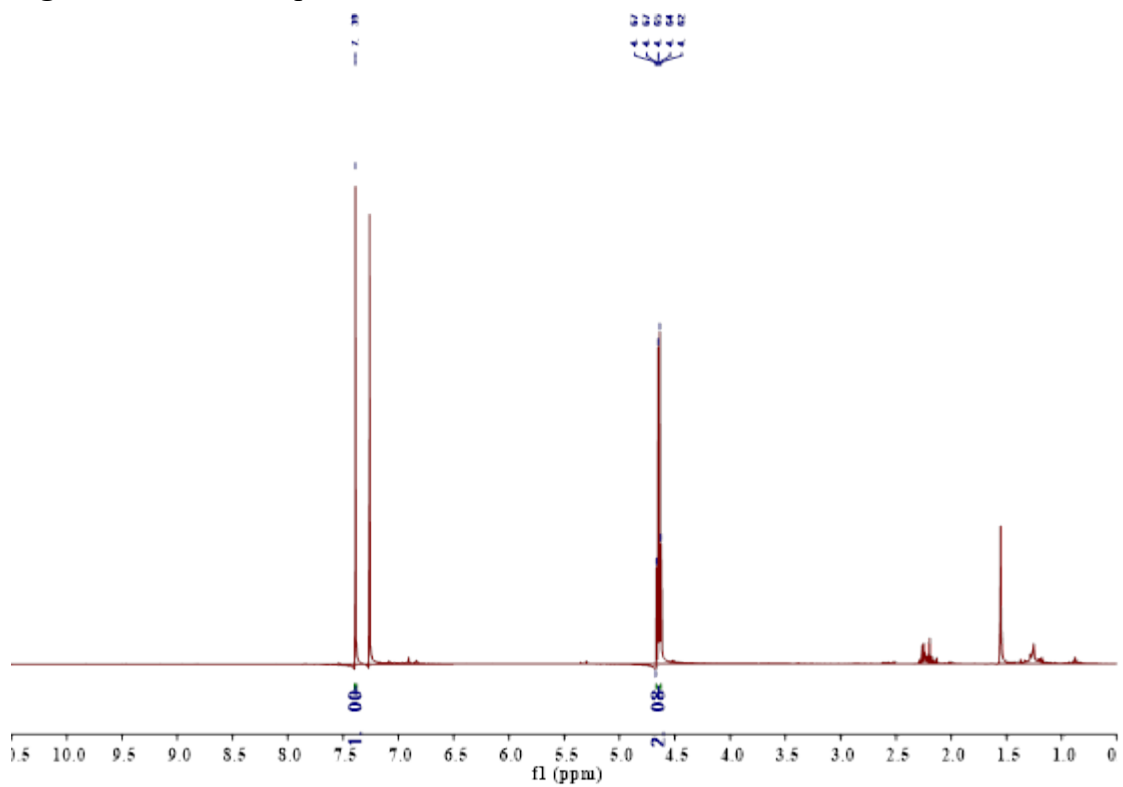


Figure S2. ¹H NMR spectrum of DBTFE.

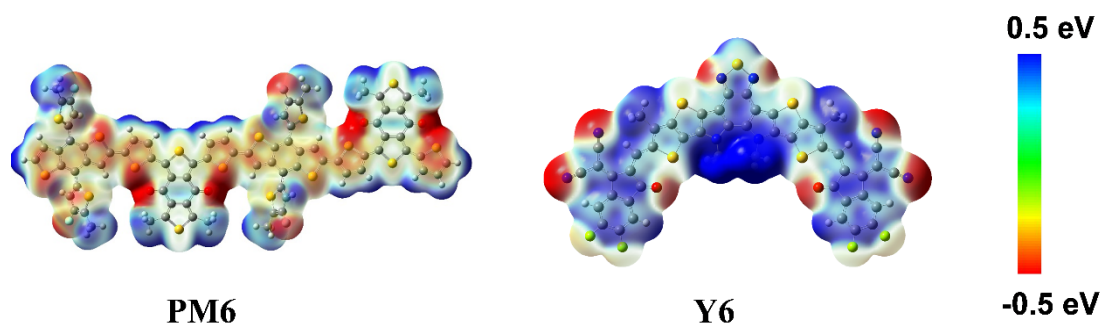


Figure S3. Calculated ESP distribution of PM6 and Y6.

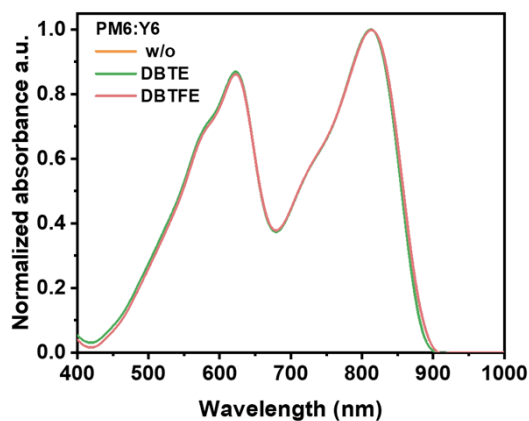


Figure S4. Normalized absorption spectra of blend films.

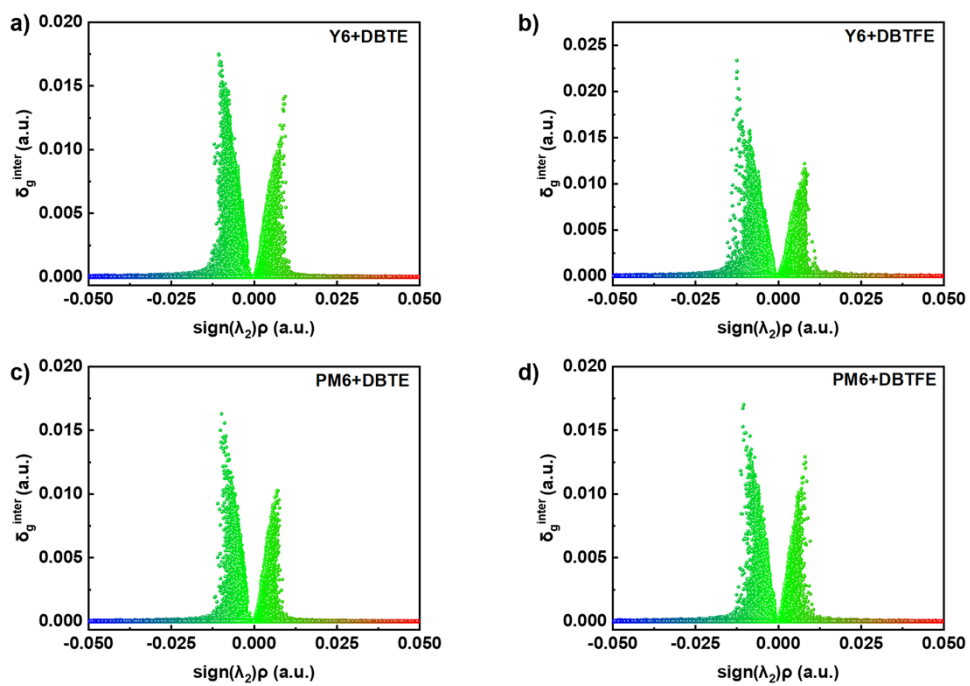


Figure S5. The IGMH scatter graphs.

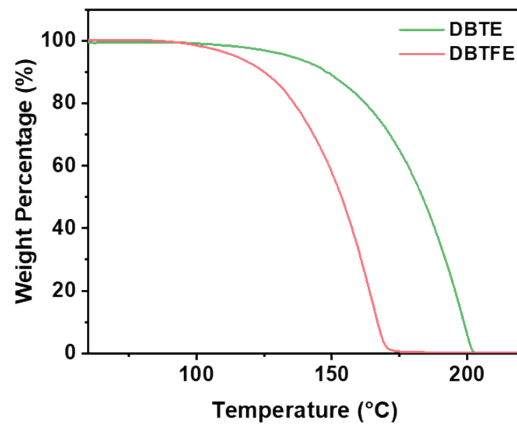


Figure S6. TGA curves of DBTE and DBTFE.

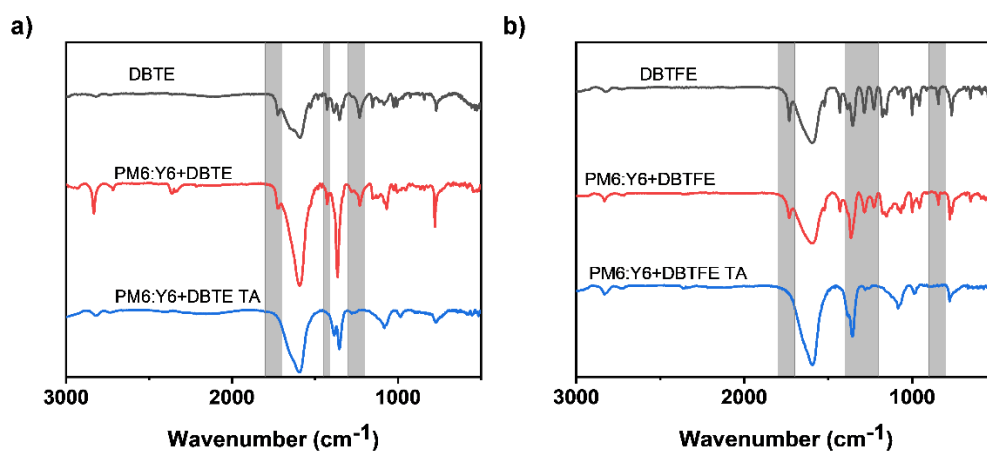


Figure S7. FTIR spectra of the additives and PM6:Y6 with/without thermal annealing.

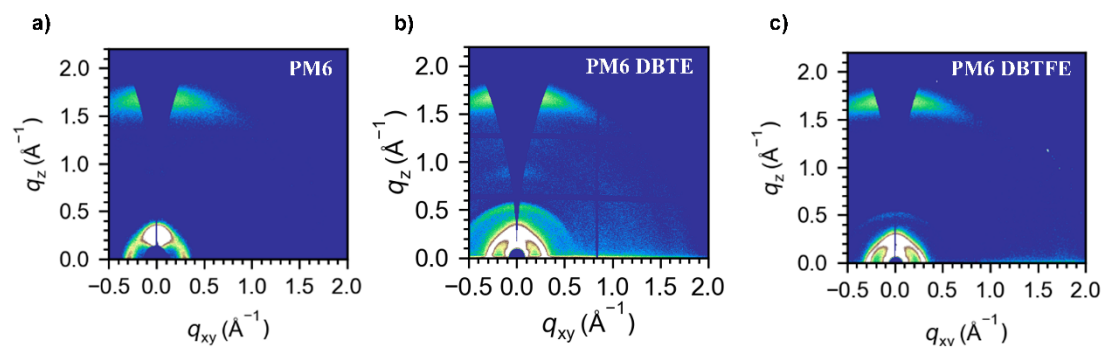


Figure S8. 2D GIWAXS patterns for neat PM6-based film (a) w/o, (b) with DBTE, (c) with DBTFE.

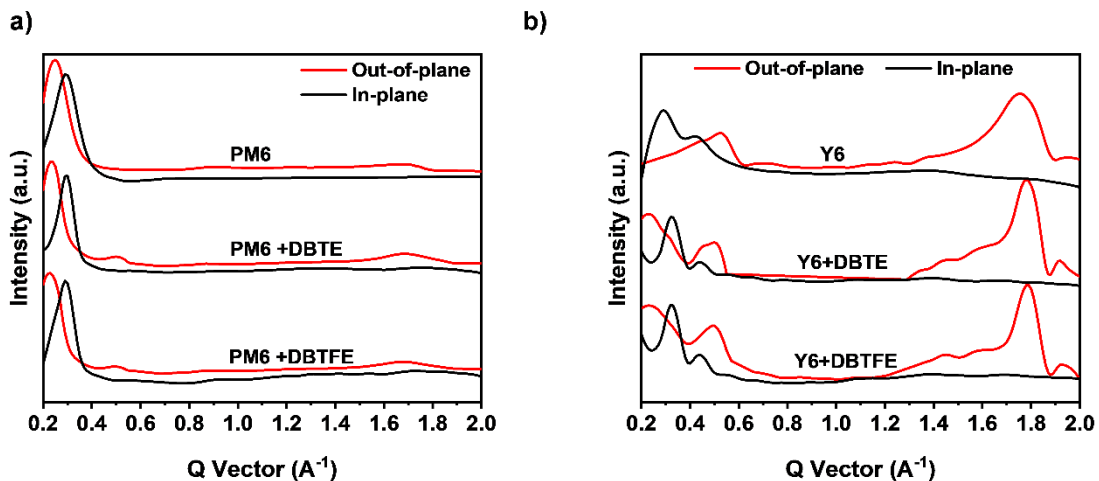


Figure S9. In-plane (black) and out-of-plane (Red) GIWAXS profiles of the corresponding PM6 (a) and Y6 (b) based pure films.

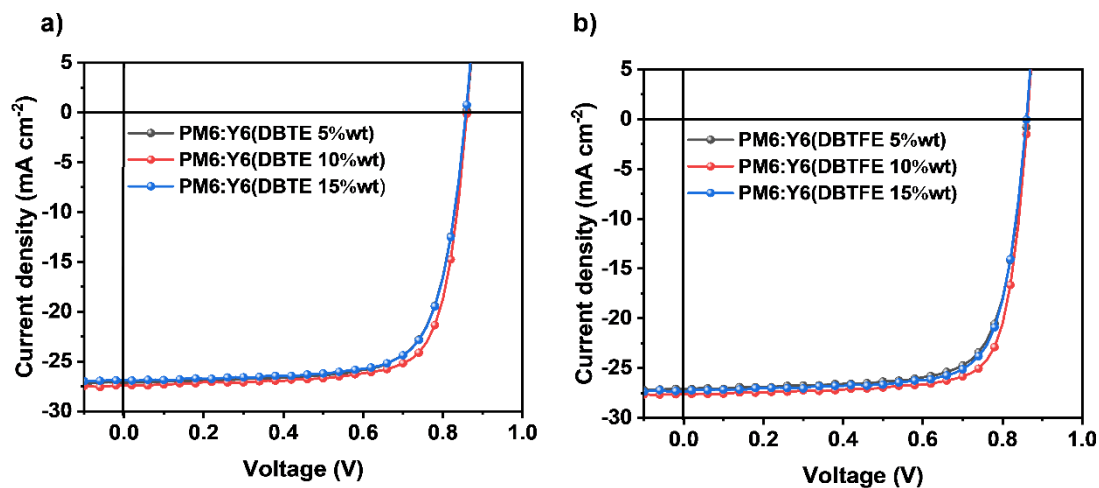


Figure S10. J - V curves of OSCs based on PM6:Y6 w/o or w/ the additives treatment.

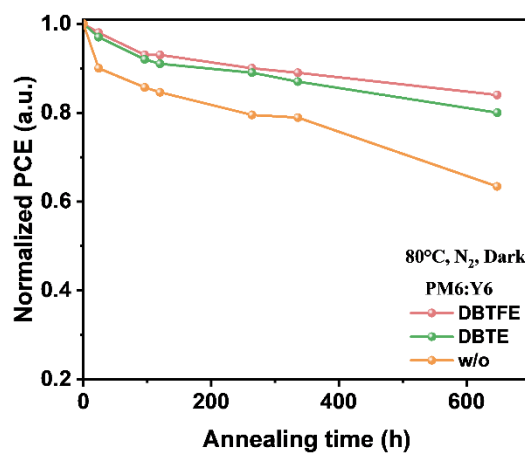


Figure S11. Normalized PCEs of the PM6:Y6 devices w/o or w/ the additives treatment as a function of exposure time in N_2 atmosphere at 80 °C.

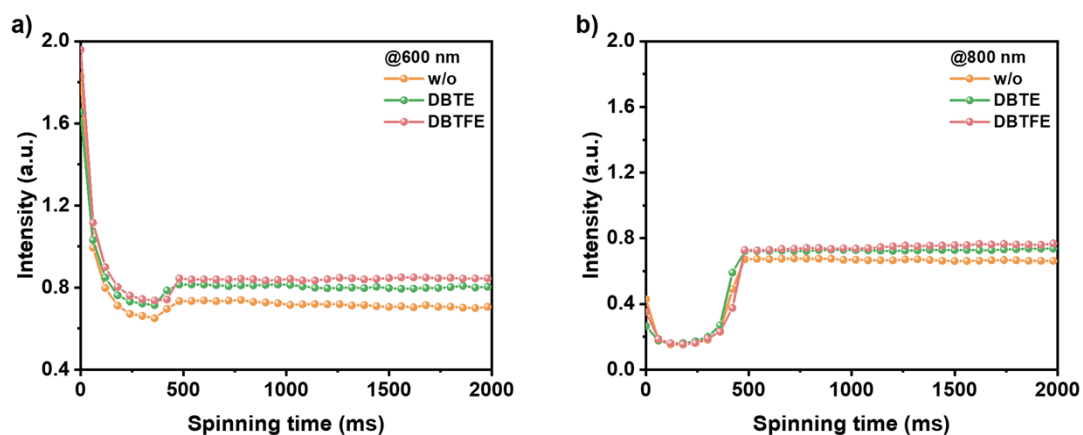


Figure S12. Absorption intensity of three types of films variation tendency as a function of spin-coating time at a) 600 nm, b) 800 nm.

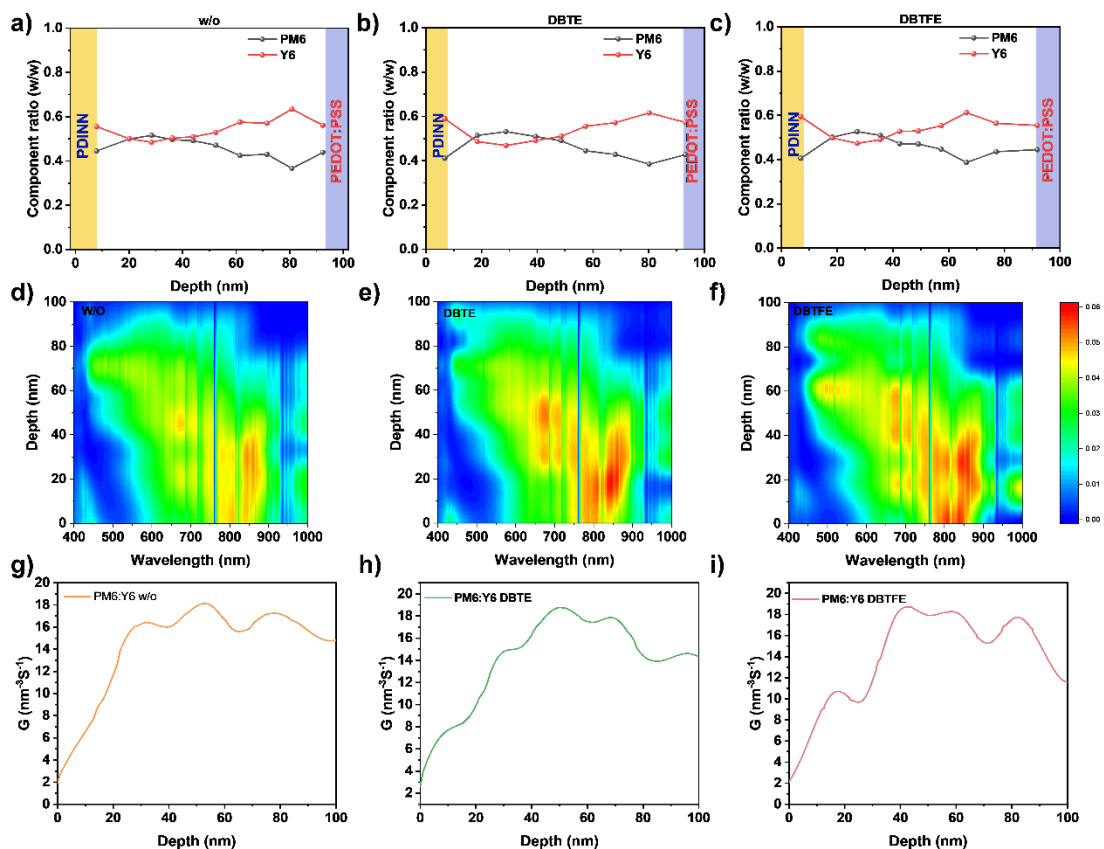


Figure S13. a-c) Component ratios with the film thickness variation. d-f) Calculated exciton generation contours of PM6:Y6-based blend films. g-i) Calculated exciton generation rate curves on the depth of the PM6:Y6-based films.

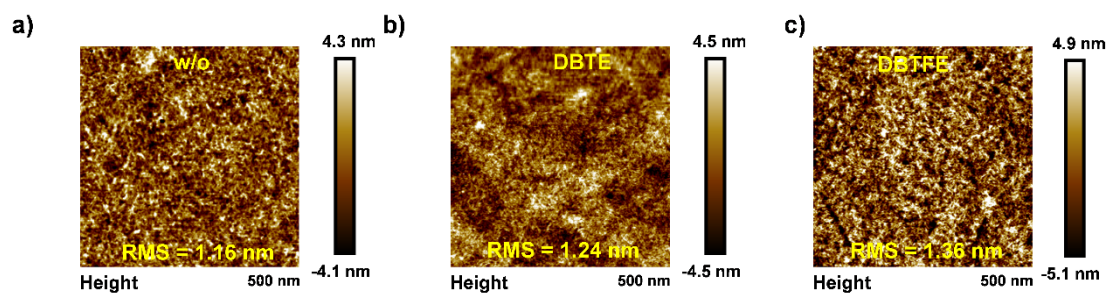


Figure S14. The AFM height images for PM6:Y6-based blend film (a) w/o, (b) with DBTE, and (c) with DBTFE.



Figure S15. Contact angle images of various films with diverse additives.

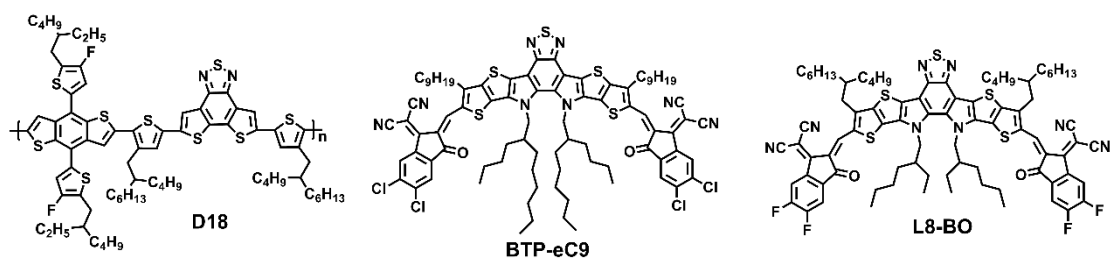


Figure S16. Chemical structures of D18, BTP-eC9, and L8-BO.

Table S1. Data of PM6 and Y6 with/without additives in the In-plane (100) and out-of-plane (010) peak analysis of GIWAXS.

Sample	Direction	Location (\AA^{-1})	D-spacing (\AA)	FWHM	CCL (\AA)
PM6	OOP	1.68	3.73	0.194	29.11
	IP	0.29	21.65	0.098	56.53
PM6(DBTE)	OOP	1.68	3.73	0.170	33.23
	IP	0.30	20.93	0.091	62.23
PM6(DBTFE)	OOP	1.68	3.73	0.182	31.12
	IP	0.30	21.28	0.093	60.87
Y6	OOP	1.75	3.59	0.194	29.20
	IP	0.29	21.51	0.077	73.40
Y6(DBTE)	OOP	1.78	3.53	0.101	55.89
	IP	0.32	19.50	0.070	80.83
Y6(DFTFE)	OOP	1.78	3.52	0.098	57.46
	IP	0.32	19.44	0.063	90.39

Table S2. Device parameters of PM6:Y6-based OSCs with different contents of additives.

Additive	PM6:Y6:additive (wt%)	V_{oc} (V)	J_{sc} (mA cm^{-2})	FF (%)	PCE (%)
w/o	1:1.2:0	0.850	26.3	72.5	16.2
	1:1.2:5	0.858	27.1	74.5	17.3
DBTE	1:1.2:10	0.858	27.4	76.2	17.9
	1:1.2:15	0.856	26.9	74.7	17.2
	1:1.2:5	0.860	27.4	75.5	17.8
DBTFE	1:1.2:10	0.861	27.6	78.2	18.6
	1:1.2:15	0.858	27.3	77.5	18.2

Table S3. Device parameters of PM6:Y6-based OSCs with different temperature of DBTFE.

Additive	Annealing Temperature (°C)	V_{oc} (V)	J_{sc} (mA cm ⁻²)	FF (%)	PCE (%)
DBTFE	90	0.860	27.5	75.5	17.9
	100	0.861	27.6	78.2	18.6
	110	0.857	27.3	77.2	18.1

Table S4. The electrical parameters of PM6:Y6-based devices.

PM6:Y6	P_{diss} (%)	P_{coll} (%)	μ_h (10 ⁻⁴ cm ² V ⁻¹ s ⁻¹)	μ_e (10 ⁻⁴ cm ² V ⁻¹ s ⁻¹)	μ_h/μ_e
w/o	93.2	81.4	3.83	3.23	1.18
DBTE	95.4	87.1	3.88	3.41	1.13
DBTFE	97.3	89.4	4.49	4.14	1.08

Table S5. Crystallization time and rate of the donor and acceptor obtained from in-situ UV measurements.

Additives	Time (ms)	
	(PM6)	(Y6)
w/o	300	360
DBTE	420	360
DBTFE	420	480

Table S6. Parameters of contact angles and surface energies of films.

Films	Contact angle(deg)		surface free energy $\gamma(\text{mJ m}^{-2})$	$\chi_{\text{donor-acceptor}}$ (K)
	H ₂ O (average)	EG (average)		
PM6	102.6	74.0	28.7	
Y6	93.2	68.0	26.5	0.09
PM6(0F)	103.8	74.8	28.0	
Y6(0F)	96.1	65.2	32.2	0.16
PM6(3F)	104.8	75.8	27.8	
Y6(3F)	97.2	64.8	34.4	0.36

Table S7. Data of PM6: Y6 with/without additives in the In-plane (100) and out-of-plane (010) peak analysis of GIWAXS.

Sample	Direction	Location (\AA^{-1})	D-spacing (\AA)	FWHM (\AA^{-1})	CCL (\AA)
PM6:Y6	OOP	1.72	3.64	0.211	26.81
	IP	0.30	21.07	0.100	56.40
PM6:Y6(DBTE)	OOP	1.73	3.63	0.190	29.79
	IP	0.30	20.86	0.084	67.25
PM6:Y6(DFTFE)	OOP	1.74	3.61	0.167	33.87
	IP	0.31	20.59	0.068	83.62